

The richness dependence of galaxy cluster correlations: Results from a redshift survey of rich APM clusters.

R.A.C. Croft^{1,2}, G.B. Dalton¹, G. Efstathiou¹, W.J. Sutherland¹
and S.J. Maddox³

¹*Department of Physics, University of Oxford, Keble Road, Oxford, OX1 3RH, UK.*

²*Department of Astronomy, The Ohio State University, Columbus, Ohio 43210, USA.*

³*Royal Greenwich Observatory, Madingley Road, Cambridge, CB3 0EZ, UK.*

1 October 2018

ABSTRACT

We analyse the spatial clustering properties of a new catalogue of very rich galaxy clusters selected from the APM Galaxy Survey. These clusters are of comparable richness and space density to Abell Richness Class ≥ 1 clusters, but selected using an objective algorithm from a catalogue demonstrably free of artificial inhomogeneities. Evaluation of the two-point correlation function $\xi_{cc}(r)$ for the full sample and for richer subsamples reveals that the correlation amplitude is consistent with that measured for lower richness APM clusters and X-ray selected clusters. We apply a maximum likelihood estimator to find the best fitting slope and amplitude of a power law fit to $\xi_{cc}(r)$, and to estimate the correlation length r_0 (the value of r at which $\xi_{cc}(r)$ is equal to unity). For clusters with a mean space density of $1.6 \times 10^{-6} h^3 \text{Mpc}^{-3}$ (equivalent to the space density of Abell Richness ≥ 2 clusters), we find $r_0 = 21.3^{+11.1}_{-9.3} h^{-1} \text{Mpc}$ (95% confidence limits). This is consistent with the weak richness dependence of $\xi_{cc}(r)$ expected in Gaussian models of structure formation. In particular, the amplitude of $\xi_{cc}(r)$ at all richnesses matches that of $\xi_{cc}(r)$ for clusters selected in N-Body simulations of a low density Cold Dark Matter model.

Key words: Galaxies : Clustering ; Large-scale structure of the Universe ; Cosmology.

1 INTRODUCTION

Rich clusters of galaxies have been used by many authors as tracers of the large-scale structure of the Universe. Most analyses to date have relied on the cluster catalogue of Abell (1958) (and later Abell, Corwin & Olowin 1989 (ACO)). Angular clustering statistics for Abell clusters were calculated by Bogart & Wagoner (1973) and Hauser & Peebles (1973) and more recently, various redshift surveys of Abell clusters have been used to estimate the two point cluster correlation function $\xi_{cc}(r)$ (eg. Bahcall & Soneira 1983, Klypin & Kopylov 1983, Postman, Huchra & Geller 1992, Peacock & West 1992). From these studies, the two point correlation function for clusters has been found to be consistent in shape with the power law form measured for galaxies,

$$\xi_{cc}(r) = \left(\frac{r}{r_0}\right)^{-\gamma} . \quad (1)$$

with a similar value of the power-law index $\gamma \sim 2$ but with a higher amplitude r_0 . For example, Peacock & West (1992) find $r_0 = 21 h^{-1} \text{Mpc}$ (where $H_0 = 100 h \text{km s}^{-1}$) for Abell clusters of richness $R \gtrsim 1$ whereas r_0 is around $5 h^{-1} \text{Mpc}$

for galaxies (see eg. Davis & Peebles 1983). Many authors have found, however, that there is much evidence to suggest that the Abell catalogue, selected by eye from unmatched photographic plates, is affected by inhomogeneities in cluster selection which result in artificial clustering (Sutherland 1988; Sutherland & Efstathiou 1991; Dekel *et al.* 1989; Peacock & West 1992).

New results on the distribution of clusters have been obtained from an automatically selected catalogue based on the APM Galaxy Survey (Dalton *et al.* 1992, hereafter DEMS92), and from smaller samples of clusters selected from the Edinburgh–Durham Galaxy Catalogue and from the ROSAT X-ray cluster survey (Nichol *et al.* 1992; Romer *et al.* 1994). The amplitude of ξ_{cc} measured from these studies is generally lower than for the Abell samples, so that $13 h^{-1} \text{Mpc} \lesssim r_0 \lesssim 16 h^{-1} \text{Mpc}$. However, it has been argued that the clustering seen in the automated surveys is dominated by poor clusters, and that the results may be compatible with the higher values of r_0 measured for $R \gtrsim 1$ Abell clusters, provided that there is a strong dependence of the correlation length on cluster richness. Bahcall & West (1992)

and Bahcall & Cen (1992) argue that the Abell data are consistent with a linear relation between r_0 and mean intercluster separation d_c ($d_c = n_c^{-1/3}$ where n_c is the mean space density) so that

$$r_0 = 0.4d_c. \quad (2)$$

The evidence for this scaling relation, especially at high values of d_c comes exclusively from estimates of the correlation functions of rich Abell clusters (eg. Peacock & West 1992). The validity of equation (2) thus depends critically on the uniformity of the Abell catalogue, particularly at richnesses $R \gtrsim 1$. The main aim of this paper is to test the scaling relation (2) using an independent sample of rich clusters of galaxies selected from the APM galaxy survey.

Croft & Efstathiou (1994) have shown that the amplitude of the cluster correlation function is predicted to vary only weakly with cluster space-density for a range of Cold Dark Matter (CDM) models. The existing data for APM clusters (Dalton *et al.* 1994a) are in good agreement with these predictions, but as the clusters are of relatively low richness and hence low d_c they are also consistent with the relationship given in Equation 2. In the study presented here we use a new extension of the APM cluster survey to test the behaviour of ξ_{cc} for richer clusters.

The layout of this paper is as follows. We describe the cluster sample and its relationship to the samples of Dalton *et al.* (1994a) and Dalton *et al.* (1994b) in Section 2. In Section 3 we present the correlation function for the new cluster sample and for various subsamples. We use a maximum likelihood estimator to fit a power law to the correlation function and investigate how the fitted parameters change with cluster richness. In Section 4 we compare our results with other data samples and with N-body simulations of cosmological models. We summarise our findings in Section 5.

2 THE CLUSTER SAMPLE

DEMS presented a summary of the algorithm used to select galaxy clusters from the APM survey. In Dalton *et al.* (1994a) the selection procedure was changed slightly in order to increase the volume available to the survey. A detailed description of the selection procedure and a discussion of the effects of changing the various selection parameters is presented in Dalton *et al.* (1997). Here we use the framework discussed in that paper to briefly describe changes to the selection procedure which increase our sensitivity to rich clusters at the expense of incompleteness at low richnesses.

The effective depths of the cluster samples selected from the APM survey are limited by the definition of the cluster richness, \mathcal{R} . This is defined to be the weighted number of galaxies in the magnitude range $[m_X - 0.5, m_X + 1.0]$ above the mean background count in the range $[m_X - 0.5, m_X + 1.5]$. Here m_X is defined as the magnitude of the galaxy for which the weighted count above background exceeds $X = \mathcal{R}/2$ for the catalogue of DEMS92 and Dalton *et al.* (1994b). The depth of the cluster catalogue defined in this way is fixed by the magnitude limit of the survey ($b_J=20.5$), so m_X is constrained to be brighter than $b_J = 19.0$. In Dalton *et al.* (1994a) we created a catalogue of greater depth by changing the background slice to $[m_X - 0.5, m_X + 1.0]$,

and redefining X to be $\mathcal{R}/2.1$. By combining this new catalogue with that of DEMS92 using a richness transformation calibrated from clusters that appear in both catalogues we created an extended sample of 364 clusters with APM richness $\mathcal{R} \geq 50$ (sample B of Dalton *et al.* 1994a). We will use results from this comparatively low richness sample in comparisons with measurements of clustering made from our new rich sample.

The new rich sample was created by further extending our survey by increasing the limiting magnitude of the galaxy catalogue to $b_J = 21.0$. The APM photometry is complete to this limit but the fraction of objects which are mis-classified as stars rises sharply. However the distribution of stellar objects fainter than $b_J=20.5$ is smooth on the scale of the counting annulus we use to determine the background correction, and so does not affect our ability to select clusters. We changed our cluster selection parameters to $X = \mathcal{R}/3$ and a richness counting slice (count and background) of $[m_X - 0.5, m_X + 0.7]$ to optimise the depth increase gained by using the extra 0.5 mag of galaxy data. We scaled the richness counts in this catalogue by matching to the sample A catalogue in the same way as for sample B (see Dalton *et al.* 1994a), and then targeted all previously unidentified clusters with $\mathcal{R} \geq 80$. In two and a half clear nights at the Anglo-Australian Telescope (AAT) we were able to obtain unambiguous redshifts for 100 new clusters. The redshifts were obtained using the cross-correlation technique of Tonry & Davis (1979). The procedure is described in detail in Dalton *et al.* (1994b).

To choose which clusters to observe, the catalogue was split into different richness subsets and these were each split further into 4 bands by RA. We were able to complete observations of the clusters in all subsets except for the poor clusters with $RA > 2$ hrs. As the efficiency of detection in our new catalogue is lowest for the poorest clusters ($\mathcal{R} \lesssim 80$, due to the change in selection parameters), most of the poor clusters in sample C are those from the previous catalogue. Because of this, we limit our final statistical sample to nearby clusters in order to have an essentially complete sample. We choose to limit the sample to those clusters with a redshift $cz \leq 55000 \text{ km s}^{-1}$. Above this redshift the overall efficiency of cluster detection appears to fall rapidly as we will show below.

Combining the cluster data with sample B gives a sample of 165 clusters with $\mathcal{R} \geq 80$ which we shall refer to as sample C. The redshift distribution of sample C is shown in panel (a) of Fig. 1, together with smoothed distribution obtained by convolving the histogram with a Gaussian of width 8000 km s^{-1} . The selection function also shown (normalised to unity at the peak) suggests that incompleteness in the deep sample starts to become important at high redshift ($cz \geq 55000 \text{ km s}^{-1}$). The peak in the $n(z)$ distribution at $cz = 60000 \text{ km s}^{-1}$ corresponds to a visible feature in the APM galaxy map at $\alpha = 23^{\text{h}}, \delta = -20^\circ$, and appears to be present in the ACO catalogue in the form of a large number of distance class 6 clusters without published redshifts. There is also a lack of clusters in sample C at low redshifts ($cz \lesssim 10000 \text{ km s}^{-1}$). This is mainly a consequence of clusters appearing too large on the plane of the sky for selection using percolation Dalton *et al.* (1997). There also do not appear to be any nearby very rich clusters in other surveys which overlap with the APM such as the SSRS galaxy

[b]

Table 1. The space density of clusters

Sample		N_c	cz_{min}	cz_{max}	$n_c (h^3 \text{Mpc}^{-3})$
B	$\mathcal{R} \geq 50$	362	5000	55000	3.4×10^{-5}
B	$\mathcal{R} \geq 70$	114	5000	55000	9.0×10^{-6}
C	$\mathcal{R} \geq 80$	163	10000	85000	5.4×10^{-6}
C	$\mathcal{R} \geq 90$	79	10000	85000	3.1×10^{-6}
C	$\mathcal{R} \geq 100$	37	10000	85000	1.8×10^{-6}
C	$\mathcal{R} \geq 110$	18	10000	85000	1.6×10^{-6}

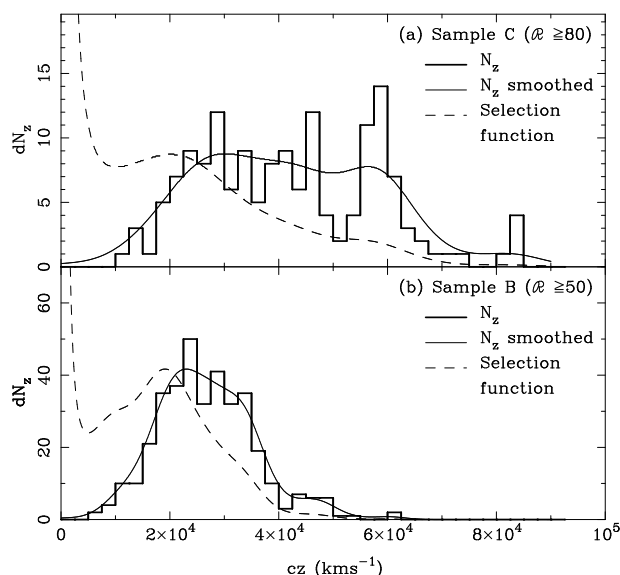


Figure 1. (a) The redshift distribution of Sample C, the new rich cluster sample. The thick lines are a histogram of the distribution of cluster redshifts, a smoothed version of which (see text) is shown by the thin solid line. The dashed line represents the selection function for the sample, obtained by dividing the smoothed distribution by the appropriate volume element. (b) For comparison, we plot dN_z for the survey of the extended sample of 364 clusters (Sample B) of Dalton *et al.* (1994a)

redshift survey (da Costa *et al.* 1994). This is a very small fraction of the volume of the rich cluster survey and in any case, we choose to limit the rest of our analysis to the clusters with $cz > 10000 \text{ km s}^{-1}$. The redshift distribution for sample B is also shown, for comparison, in panel (b) of Fig 1. The smoothing of the distribution in this case was carried out using 4000 km s^{-1} Gaussian because of the higher space density of objects.

We have estimated the mean space density of clusters in this sample, using Equation 3 of Efstathiou *et al.* (1992) and the results are given in Table 1. We have also applied successively higher richness bounds to create subsamples with lower space densities, the estimated space densities as listed in Table 1. We also list the space density of sample B and a subsample with $\mathcal{R} \geq 70$.

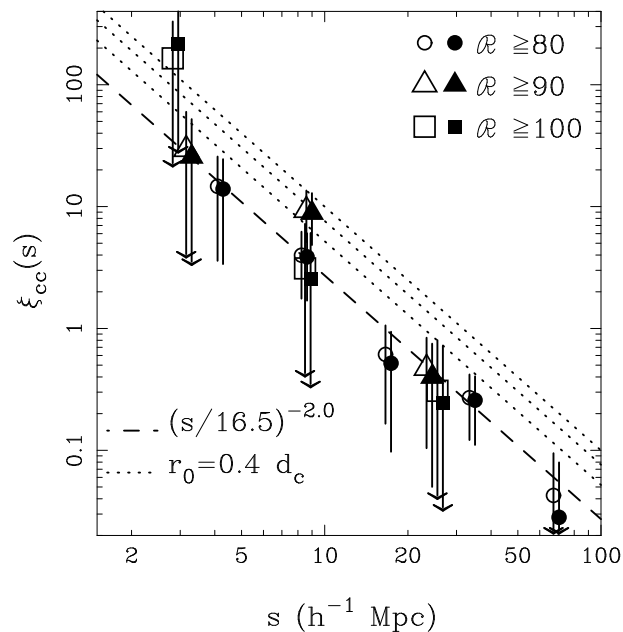


Figure 2. The two-point correlation function for the three sub-samples of clusters from sample C, as discussed in the text. The estimator of equation (4) was used to calculate the solid symbols and equation (3) for the open symbols (which have been displaced to the left slightly to make the error bars visible). The dashed line represents the best fit to the data for $\mathcal{R} \geq 80$, $\xi_{cc} = (s/16.5 h^{-1} \text{Mpc})^{-2.0}$. The dotted lines show the prediction of equation (2) for the power-law fits to the correlation function of each of the sub-samples.

3 CLUSTER CORRELATIONS

We estimate the redshift-space correlation functions for the samples in Table 1 by cross-correlating with a random catalogue and using the estimator

$$\xi_{cc}(s) = 2f \frac{DD}{DR} - 1, \quad (3)$$

where DD and DR are the number of cluster-cluster pairs and the number of cluster-random pairs respectively in each bin centred on s . The parameter f is the ratio of the number of random points to the number of clusters in the sample. In each case we use 20,000 points distributed within the survey boundaries and with the same redshift distributions as the smoothed distributions shown in Figure 1. As stated in section (2), we present results for the clusters with $cz \leq 55000 \text{ km s}^{-1}$ in order to be minimise any effects that are due to uncertainty in the selection function at high redshift. This being the case, we have also studied the clustering of the full sample and in all cases find the measurements to lie within 1σ of the $cz \leq 55000 \text{ km s}^{-1}$ sample results.

We also use the estimator of Hamilton (1993):

$$\xi_{cc}(s) = 4 \frac{(DD)(RR)}{(DR)^2} - 1, \quad (4)$$

which is less affected by uncertainties in the selection function for $\xi_{cc} < 1$.

To test the dependence of the correlation function on cluster space density we estimate $\xi_{cc}(r)$ for subsamples with $\mathcal{R} \geq 90$ and $\mathcal{R} \geq 100$. In Figure 2 we show the correlation

functions for the full sample and for these subsamples. We note that for the $\mathcal{R} \geq 100$ clusters each point is within 1σ of zero. A least-squares fit to the data (using estimator (3)) for $\mathcal{R} \geq 80$ yields $\gamma = 2.0 \pm 0.4$ and $A = 10^{2.4 \pm 0.44}$ where $A = r_0^\gamma$, and the quoted errors are 1σ . This gives $r_0 = 16.5 h^{-1}\text{Mpc}$. If the slope is constrained to be $\gamma = 2.0$ we find $r_0 = 16.5_{-6.0}^{+7.0} h^{-1}\text{Mpc}$ where the errors are calculated from the 5 percentile points of the χ^2 distribution. The best fit power law for the $\mathcal{R} \geq 90$ subsample is steeper, with $\gamma = 2.8 \pm 1.0$, $A = 10^{3.8 \pm 1.0}$. If γ for this subsample is constrained to be 2.8, then we obtain $r_0 = 19.1_{-7.5}^{+8.0} h^{-1}\text{Mpc}$.

The fit for $\mathcal{R} \geq 80$ is shown as the dashed line in Figure 2. The data for the $\mathcal{R} \geq 100$ and $\mathcal{R} \geq 90$ sample appear to be in reasonable agreement with the $\mathcal{R} \geq 80$ sample. We have plotted the predictions of equation (2) for the correlation functions of the different samples. Most of the points lie below the corresponding prediction. We therefore conclude that the correlation amplitude is not strongly dependent on the cluster richness.

3.1 A maximum likelihood estimator of γ and r_0 .

As we are interested in the behaviour of r_0 as a function of cluster richness, we would like to be able to estimate its value and error bounds in the most direct way possible. Binning the data introduces uncertainties, as the value of $\xi(r)$ can depend on the binning interval and the position of bin centres (in log or linear space). We circumvent these problems by maximising the likelihood that a power law form for $\xi(r)$, as in equation (1) will produce the observed set of pair separations. In this way, we can find confidence limits on the two parameters γ and r_0 , even for small numbers of clusters.

To construct our estimator, we need to find the predicted probability distribution of cluster pairs for each value of γ and r_0 . We deal with the mask and selection function in the usual way by creating a catalogue of random points with the same boundaries and selection function as the cluster catalogue in question. We then calculate the separations of all the cluster-random pairs and bin them in r . The bin width can be made arbitrarily small as long as number of points in the random catalogue is increased accordingly. In this case we use 100000 random points in the catalogue and 200 bins in the interval $0 - 100 h^{-1}\text{Mpc}$. If the number of cluster-random pairs in an interval dr is $g(r)dr$, then the predicted mean number of cluster-cluster pairs in that interval is $h(r)dr$ where

$$h(r)dr = f(1 + \xi_{cc}(r))g(r)dr, \quad (5)$$

f is the number of clusters divided by the number of random points, and $\xi_{cc}(r)$ has the power law form given by Equation 1. We can then use the separations (r_i) of all the (N) cluster-cluster pairs to form a likelihood function \mathcal{L} . \mathcal{L} is defined as the product of the probabilities of having exactly one pair in the interval dr at each of the pair separations r_i of the N pairs and the probability of having zero pairs in all the other differential elements of r . This is for all r in a chosen range (say r_a to r_b), in our case the range of values for which $\xi_{cc}(r)$ can be reasonably expected to have power law behaviour. To find the likelihood, we assume Poisson probabilities, so that (see also Marshall *et al.* 1983):

$$\mathcal{L} = \prod_i^N e^{-\mu} \mu \prod_{j \neq i} e^{-\mu}, \quad (6)$$

where $\mu = h(r)dr$, the expected number of pairs in the interval dr , and the index j runs over all the elements dr in which there are no pairs. We then define the usual quantity $S = -2 \ln \mathcal{L}$ and drop all terms independent of model parameters, so that

$$S = 2 \int_{r_a}^{r_b} h(r)dr - 2 \sum_i^N \ln(h(r_i)). \quad (7)$$

The best fit values of r_0 and γ are obtained by minimising S , with confidence levels defined by $\Delta_S = S(r_{best}, \gamma_{best}) - S(r_0, \gamma)$, assuming that Δ_S is distributed with a χ^2 distribution. These confidence limits are likely to be underestimates, as the assumption of Poisson statistics assumes that all pairs are independent of each other. It may be possible to incorporate the effects of higher order correlations into the likelihood by using a scaling model for the three point and higher correlation functions (see e.g. Peebles 1980). This would result in more accurate error bars. However, we can use N-body simulations to give us an idea of the real errors. Croft & Efstathiou (1994) compared error bars on the individual points obtained using Poisson statistics with the scatter between results for different simulated cluster surveys. In that case, the ensemble errors, which include the additional effects of cosmic variance were between 1.3 and 1.7 times larger than the Poisson errors. We expect the errors computed from our likelihood analysis to be underestimates by roughly the same factor. We check here whether this is the case by using large box size N-body simulations (see Section 4) to make simulated cluster catalogues with the same angular shape and selection function as sample C and richer subsamples selected from it (see Section 3). We have done this for the low density CDM model (see Section 4) for which 10 simulations are available. In Table 2 we present the values of r_0 and γ and their 1σ confidence intervals ($(\delta_{r_0})_i$ and $(\delta_\gamma)_i$) obtained by applying the maximum likelihood estimator to the simulated catalogues. Also shown is the ratio of these errors to the ensemble errors ($\sigma(r_0)$ and $\sigma(\gamma)$). From these results we can see that our expectations are approximately correct and that the likelihood errors are underestimates by between 1.1 and 2.1. We can also see that the Poisson errors are closer to the real errors when the number of clusters is small. Our estimates of the error bars for the richest subsamples of clusters should therefore be the most accurate.

3.2 γ and r_0 from APM clusters and the richness dependence of r_0 .

We apply the estimator described above to the catalogue C subsample of 110 rich APM clusters with $cz < 55000\text{km s}^{-1}$ as well as subsamples with varying lower richness bounds. From consideration of the plot of $\xi_{cc}(r)$ in bins for the full sample, as well as the results for sample B of Dalton *et al.* (1994a), we decide that $\xi_{cc}(r)$ can probably be fitted to a power law over the range $r_a = 2 h^{-1}\text{Mpc}$ to $r_b = 70 h^{-1}\text{Mpc}$. Varying these limits does not greatly affect the results, although if r_b is increased to much over

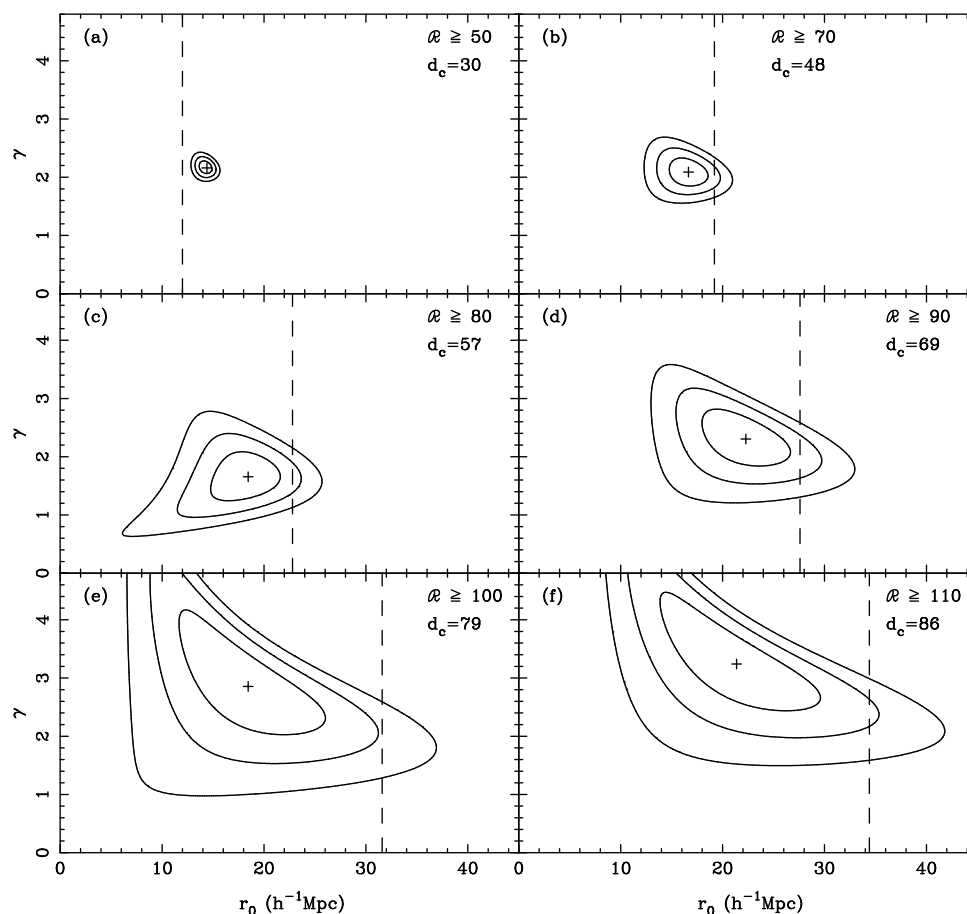


Figure 3. Contours resulting from maximum likelihood analysis of cluster pair separations in order to find the most probable values of r_0 and γ . The best fit values of these two parameters are shown by a cross in each plot. The contours enclose 68%, 95% and 99.7% of the joint probability respectively, if the distribution of $S = -2 \ln \mathcal{L}$ follows a χ^2 distribution with 2 degrees of freedom. The different panels show results for different subsamples of clusters, with varying lower richness limits. Panel (a) shows results for the extended sample of 364 clusters of Dalton *et al.* (1994a). Panel (b) shows results for the clusters in sample B with $\mathcal{R} \geq 80$. In panels (c) to (f) we use the new rich sample (C) that forms the subject of this paper. In each case the lower richness limit and the resulting mean intercluster separation d_c are shown in the top right of the panel. The dashed lines show the relation $r_0 = 0.4d_c$ of Bahcall & West (1992).

[b]

Table 2. Errors estimated from the likelihood distribution compared to the scatter between 10 simulations of a low density CDM universe. The errors on γ and r_0 are the average of the 1σ confidence intervals ($(\delta_{r_0})_l$ and $(\delta_\gamma)_l$) obtained by applying the maximum likelihood method to 10 simulated catalogues. The standard deviations of the measurements taken from the simulated catalogues are denoted by σ_{r_0} and σ_γ .

$h^{-1}\text{Mpc}$ d_c	$h^{-1}\text{Mpc}$ $r_0 \pm 1\sigma$	$(\delta_{r_0})_l/\sigma(r_0)$	$\gamma \pm 1\sigma$	$(\delta_\gamma)_l/\sigma(\gamma)$
57	$17.2^{+1.5}_{-1.6}$	0.48	$1.97^{+0.20}_{-0.20}$	0.76
69	$18.1^{+2.8}_{-3.4}$	0.60	$1.93^{+0.36}_{-0.36}$	0.90
79	$18.2^{+5.2}_{-6.7}$	0.88	$1.94^{+0.70}_{-0.73}$	0.93

70–80 $h^{-1}\text{Mpc}$, the fitted power law steepens slightly, probably due to a break in $\xi_{cc}(r)$.

We also apply the estimator to sample B, the results

for which are shown in the first panel of Figure 3. In this case, we find $r_0 = 14.2^{+0.8}_{-1.0} h^{-1}\text{Mpc}$ and $\gamma = 2.13^{+0.16}_{-0.14}$ where the errors indicate the 95% confidence bounds on each parameter individually. The contours on the plot show the joint confidence bounds at levels of 68%, 95% and 99.7%. If we choose to constrain $\gamma = 2.13$ and find the maximum likelihood value of r_0 in one dimension we also get $r_0 = 14.2^{+0.8}_{-1.0} h^{-1}\text{Mpc}$ at 95% confidence. The χ^2 fits to the binned $\xi(r)$ give $\gamma = 2.05^{+0.20}_{-0.20}$ (2σ errors). If the slope is constrained to have this value, then from the binned data $r_0 = 14.3^{+2.5}_{-2.25} h^{-1}\text{Mpc}$ (Dalton *et al.* 1994a). The errors on r_0 obtained from the binned data are therefore a factor of 2 larger than the errors from the maximum likelihood technique.

We have investigated a few possible reasons for this discrepancy. The main reason appears to be an anomalously low χ^2 for the power law fit. Fitting to the 7 bins above 2 $h^{-1}\text{Mpc}$ we find $\chi^2 = 1.7$, which should only occur $\sim 10\%$ of the time. The binned data for the richer subsamples have

more normal values of χ^2 and errors much closer to the maximum likelihood values. In discussing our results we will concentrate our attention on the fit parameters derived using the maximum likelihood method.

We have applied the maximum likelihood method to a subsample of clusters from sample B with $\mathcal{R} \geq 70$, with the results shown in Figure 3(b). These clusters have a mean separation $d_c = 48 h^{-1}$ Mpc and have a slightly larger value of $r_0 = 16.6 \pm 2.6 h^{-1}$ Mpc. We tabulate the best fit parameters γ and r_0 for this and all the other cluster samples in Table 3. We also present the 1σ and 2σ confidence limits on each parameter taken individually.

The results for sample C and subsamples of higher richness are shown in Figure 3(c)-(f). These subsamples are the same as those used in calculating the binned correlation functions plotted in Figure 2, with the addition of a subsample of APM clusters with $\mathcal{R} \geq 110$. The APM $\mathcal{R} \geq 110$ clusters have a similar space density to Abell $R \geq 2$ clusters (see e.g. Peacock & West 1992). We also plot a dashed line showing the relation $r_0 = 0.4d_c$ of Bahcall & West (1992).

We can see from the contour plots that there is a slight anticorrelation of r_0 and γ , so that lower values of r_0 would result in a steeper slope for $\xi_{cc}(r)$. As the errors are large, the value of $\gamma = 2.1$ obtained for sample B with 364 clusters is broadly compatible with γ for the rich sample, C. The slope of $\xi_{cc}(r)$ seems to be steeper than that normally quoted for the correlation function of galaxies ($\gamma \simeq 1.8$ see eg. Davis & Peebles 1983).

4 DISCUSSION

4.1 Comparison with results for other cluster catalogues.

A plot of r_0 versus d_c for various observational samples of clusters including the APM samples (taken from Table 2 above and DEMS92 and labelled APM and APM92 respectively), is shown in Fig 4. For the maximum likelihood points, the errors are 1σ for marginalisation of r_0 over all values of γ . The APM92 points are for γ constrained to be 2.0. The points labelled ‘Abell’ indicate the results for Abell $R \geq 0$, Abell $R \geq 1$ and Abell $R \geq 2$ clusters derived by Peacock & West (1992). The point labelled EDCC is the result for 79 clusters from the Edinburgh-Durham Cluster Catalogue of Lumsden *et al.* (1992) estimated by Nichol *et al.* (1992). The error bar size was estimated using bootstrap resamplings. The same is true of the error on the point labelled X-Abell, which was estimated by Nichol, Briel & Henry (1994), from 67 clusters in the redshift sample of Huchra *et al.* (1990) which also have X-ray luminosities $\geq 10^{43}$ erg s $^{-1}$. The point labelled ROSAT shows r_0 for $\xi_{cc}(r)$ measured from a redshift survey of an X-ray flux limited sample of clusters (Romer *et al.* 1994). The X-ray flux for both these last samples was measured using the ROSAT satellite.

It can be seen that most of the data points are for cluster samples with d_c in the range $30 - 55 h^{-1}$ Mpc, and that in this range, the results for the X-ray samples and automated galaxy surveys are in agreement with one another, and lower than those for Abell clusters. As has been detailed previously, this can be understood as being due to

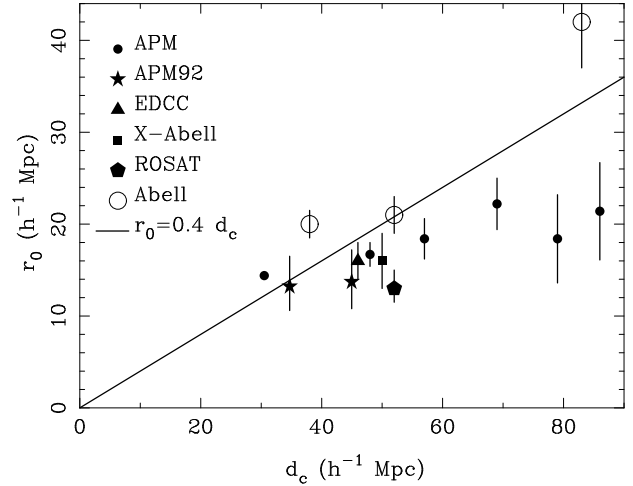


Figure 4. The quantity r_0 (the correlation length) plotted against cluster space density for a number of observed cluster samples (see text). Error bars represent the 1σ error on the mean. The solid line shows the relation $r_0 = 0.4d_c$ of Bahcall & West (1992).

non-uniformities in the Abell catalogue which artificially boosts the amplitude of clustering. Over this small range in cluster space density, for which the errors are comparatively small, there is not much evidence for any trend of r_0 with d_c and hence cluster richness. Part of the reason for the work in this paper was to find out whether this is also true at higher richnesses and lower space densities. The solid line in the plot corresponds to the scaling relation $r_0 = 0.4d_c$ proposed by Bahcall & West (1992) as a fit to the correlation functions of the Abell sample. As can be seen from the plot, the motivation for assuming this fit at high values of d_c was provided by the results for Abell $R \geq 2$ clusters (a sample of 42 clusters was used to calculate this data point – see Peacock & West 1992).

Now that we have a sample of very rich clusters taken from a catalogue which is demonstrably free of artificial inhomogeneities, we are in the position to test equation (2) using the APM data alone. The three APM points on the right of the plot are for $\mathcal{R} \geq 90$, $\mathcal{R} \geq 100$ and $\mathcal{R} \geq 110$ clusters, which have space densities comparable to that of the Abell $R \geq 2$ clusters. If the error bars are taken at face value, then the relation would appear to be ruled out at the $\sim 2\sigma$ level. However, as we have seen from Table 1, the error bars could be underestimates by a factor of $\sim 1.1 - 2.1$. Also, the space densities of clusters used to derive d_c values are not precise estimates because of the difficulties involved in estimating the completeness of richness limited cluster catalogues (see Efstathiou *et al.* 1992). That said, we believe that these data points are more reliable than those for the Abell $R \geq 2$ clusters. Table 2.1 also shows us that the error bars for the richest sub-samples are likely to be the most accurate. In summary, the APM points are consistent with a weak dependence of clustering on richness. We find no evidence that equation (2) applies to rich clusters of galaxies, with important implications for theories of structure formation as described in the next section.

[t]

Table 3. r_0 vs. d_c for different samples of APM clusters.

Sample		Number of clusters	$h^{-1}\text{Mpc}$ d_c	$h^{-1}\text{Mpc}$ $r_0 \pm 1\sigma$	$h^{-1}\text{Mpc}$ $r_0 \pm 2\sigma$	$\gamma \pm 1\sigma$	$\gamma \pm 2\sigma$
B	$\mathcal{R} \geq 50$	364	30	$14.2^{+0.4}_{-0.6}$	$14.2^{+0.8}_{-1.0}$	$2.13^{+0.09}_{-0.06}$	$2.13^{+0.16}_{-0.14}$
B	$\mathcal{R} \geq 70$	114	48	$16.6^{+1.3}_{-1.3}$	$16.6^{+2.6}_{-2.6}$	$2.1^{+0.2}_{-0.2}$	$2.1^{+0.3}_{-0.3}$
C	$\mathcal{R} \geq 80$	110	57	$18.4^{+2.2}_{-2.4}$	$18.4^{+4.2}_{-5.1}$	$1.7^{+0.3}_{-0.3}$	$1.7^{+0.6}_{-0.6}$
C	$\mathcal{R} \geq 90$	58	69	$22.2^{+2.8}_{-2.8}$	$22.2^{+6.0}_{-5.5}$	$2.3^{+0.3}_{-0.3}$	$2.3^{+0.7}_{-0.7}$
C	$\mathcal{R} \geq 100$	29	79	$18.4^{+4.8}_{-4.8}$	$18.4^{+10.2}_{-8.4}$	$2.8^{+0.8}_{-0.6}$	$2.8^{+1.8}_{-1.1}$
C	$\mathcal{R} \geq 110$	17	86	$21.3^{+5.3}_{-5.3}$	$21.3^{+11.1}_{-9.3}$	$3.2^{+0.8}_{-0.6}$	$3.2^{+1.6}_{-1.1}$

4.2 Comparison with model predictions.

Croft & Efstathiou (1994) examined the behaviour of r_0 with d_c expected in several popular cosmological scenarios (see also Bahcall & Cen 1992, Mann, Heavens & Peacock 1993). The box size ($300 h^{-1}\text{Mpc}$) of the dissipationless N-body simulations used in that study, meant that the predictions did not extend to the large values of d_c needed to make comparisons with our new rich cluster sample. We have therefore run a set of simulations (using the same particle-particle particle-mesh N-body code) with box size $600 h^{-1}\text{Mpc}$ and 4×10^6 particles. These simulations are the same as those used in Croft & Efstathiou (1995). The models we shall consider are the Standard CDM model (SCDM has $\Gamma = \Omega h = 0.5$ and $\Omega = 1$) and the spatially flat Low density CDM model (LCDM has $\Gamma = 0.2$, $\Omega = 0.2$ and $\Omega_\Lambda = 0.8$). Both models are normalised to be compatible with the first year COBE anisotropies (Wright *et al.* 1994) so that $\sigma_8 = 1.0$ for both models, where σ_8 is the rms amplitude of linear fluctuations in $8 h^{-1}\text{Mpc}$ spheres. The results are insensitive to the precise value of σ_8 . We use the same techniques as in Croft & Efstathiou (1994) and Dalton *et al.* (1994a) to find clusters in the simulations. This involves finding cluster centres in real space with a percolation algorithm and then ordering clusters by the mass contained within a certain radius, in this case $0.5 h^{-1}\text{Mpc}$. We then calculate r_0 for clusters with different lower mass limits, with the results shown in Figure 5. We have chosen to calculate the correlation functions in redshift space, for more accurate comparison with the observations. The values of r_0 which we present below are $\sim 1 h^{-1}\text{Mpc}$ larger than the values estimated in real space.

The correlation functions for the LCDM model are shown in Figure 5, together with the APM points (estimated using Equation 4). The space densities of the simulated clusters were selected to be close to those for the three subsamples of rich APM clusters plotted. The curves plotted are the averages of results for 10 simulations of LCDM. We can see that the APM results are compatible with LCDM model. We can also see that the clustering strength of LCDM clusters increases only a small amount as the richness bound is increased.

In order to see how the clustering results are affected by the mask and selection function, we have plotted the results for the mock APM cluster catalogues constructed from 10 LCDM simulations and described in Section 3.1. The results are shown in Figure 6 in the form of a scatter plot. In each

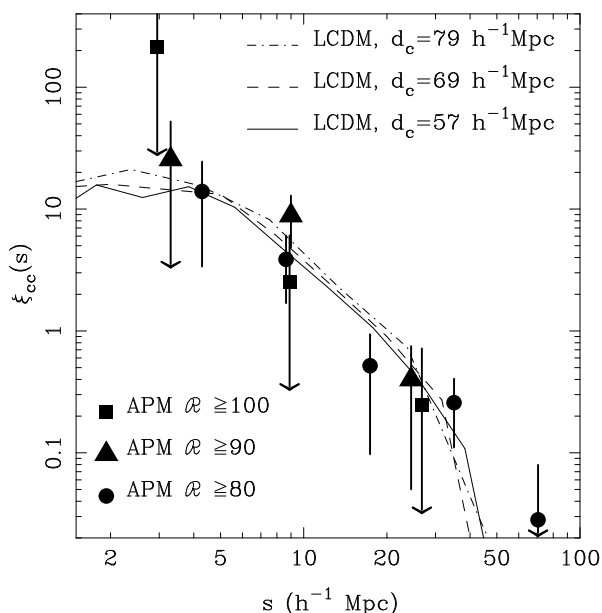


Figure 5. The two-point correlation function of simulated clusters in the LCDM model in redshift space for subsamples with three different mean separations. The APM results from Figure 2 (solid symbols, computed using the estimator of Equation 4) are also shown.

panel we plot r_0 against γ (both measured from the maximum likelihood technique). We show results calculated from clusters with the same d_c values as those in Figure 5. We also plot points for the APM results for equivalent richness clusters. In each of the panels we can see that the APM results are not extreme outliers and it looks plausible that they could have been drawn from the same distribution as the LCDM points. A line denoting the relationship of Equation 2 is drawn on each panel. From this we can conclude that in an LCDM Universe we would have a $\sim 10\%$ chance for each richness cut of measuring a value of r_0 which fits this relationship.

In Figure 7 we plot r_0 measured from the correlation functions of the LCDM and SCDM clusters against d_c . The error bars on the simulation points were calculated from the 1σ error on the mean taken from 3 simulations of each model. We therefore have 2.4 times as many clusters of any given space density as in the ensembles of Croft & Ef-

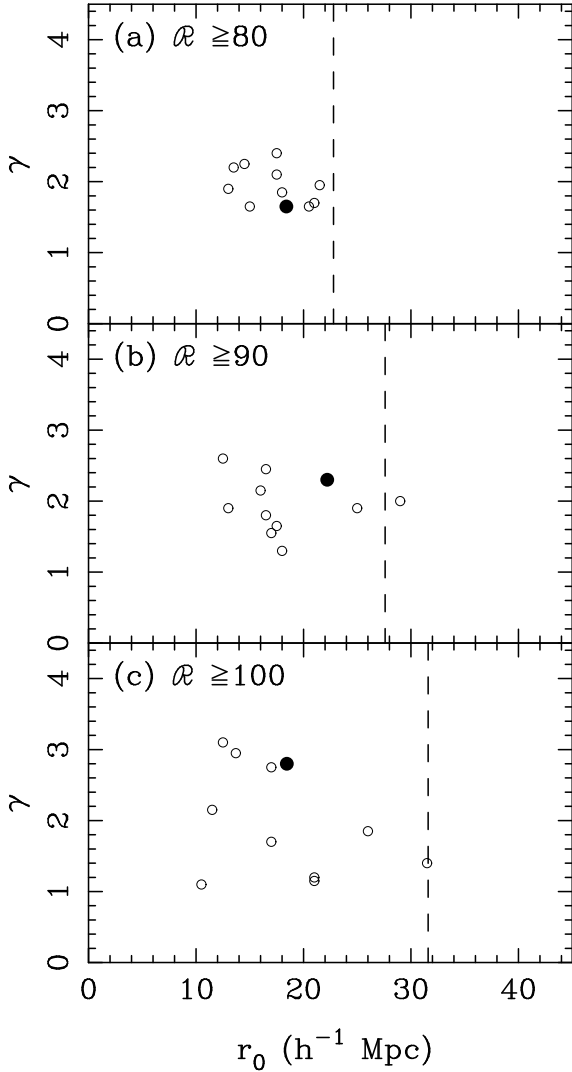


Figure 6. Values of r_0 and γ measured from mock catalogues constructed from 10 simulations of an LCDM universe (see text). Plotted are results for clusters with three different mean separations. The corresponding APM results from Figure 3. are also shown.

stathiou (1994). We also plot the values of r_0 calculated using the maximum likelihood method in this paper. The plots show the very weak trend of clustering strength with cluster richness continuing for both models at least up to $r = 80 h^{-1}\text{Mpc}$. The APM points are consistent with the LCDM model, but not with SCDM. We note here that a simulation with a different amplitude of clustering in the underlying mass could have an r_0 which differs by as much as $1 - 3 h^{-1}\text{Mpc}$ as could clusters which are selected using a different method. These variations are not expected to be large enough to affect our conclusions (Croft & Efstathiou 1994, Eke *et al.* 1996, Mo, Jing & White 1996).

It is encouraging that models with $\Gamma \approx 0.2$, which were introduced to explain clustering in the galaxy distribution (see eg. Efstathiou, Sutherland & Maddox 1990) are also able to match well the clustering of rare and extreme objects such as the rich galaxy clusters considered here. We also

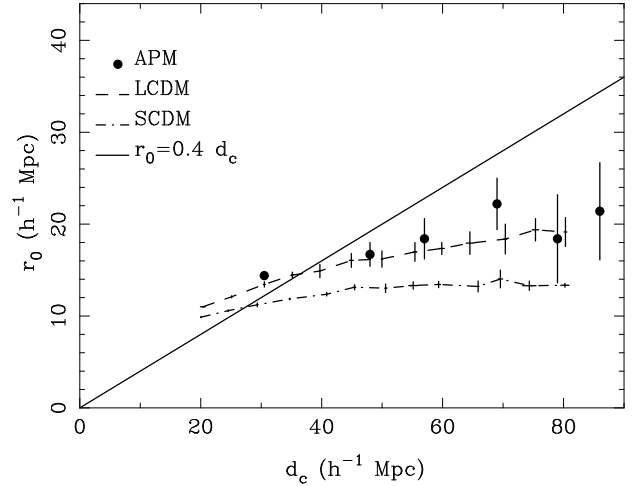


Figure 7. A comparison of the richness dependence of APM cluster correlations (filled circles) with the corresponding predictions for a low density CDM Model (dashed line) and Standard CDM (dot-dashed) line. The theoretical predictions have been calculated in redshift space. Error bars represent the 1σ error on the mean. The solid line shows the relation $r_0 = 0.4d_c$ of Bahcall & West (1992).

expect other Gaussian models with similar power spectra such as a Mixed Dark Matter (MDM) universe dominated by CDM and with an additional component of massive neutrinos (see eg. Klypin *et al.* 1993) to be compatible with our APM results at high richnesses, as they are at low richnesses (Dalton *et al.* 1994a). From Figure 7 we can also see that whilst models such as low density CDM provide a good fit to the clustering behaviour of rich APM clusters they are completely incompatible with the scaling relation derived from considering rich Abell clusters. Our data exclude such a strong scaling relation and remove the need to resort to non-Gaussian models for the formation of large-scale structure.

5 SUMMARY

We have carried out a new extension of the APM cluster redshift survey to provide a sample of 165 clusters with richnesses $\mathcal{R} \geq 80$ and mean space density of $5.4 \times 10^{-6} h^{-1}\text{Mpc}^{-3}$. The correlation function of this sample is found to be consistent with the clustering amplitude measured for our previous larger sample of poorer APM clusters. Restricting the evaluation of $\xi_{cc}(r)$ to even richer subsamples shows that there is only a weak dependence of correlation length with cluster richness. This disagrees with results from Abell $R \geq 2$ clusters. The high amplitude of ξ_{cc} for the Abell $R \geq 2$ sample is most probably caused by inhomogeneities in the Abell catalogue. The weak dependence of clustering strength with richness that we find in the APM survey is however in good agreement with what is expected in a universe with Gaussian initial fluctuations and a power spectrum with more large-scale power than standard CDM, such as low density CDM or MDM.

ACKNOWLEDGMENTS

We thank Steve Warren and Enrique Gaztañaga for helpful discussions. We also thank the staff of the AAO for hospitality and efficient observing. This work was supported by grants from the UK Particle Physics and Astronomy Research Council. RACC acknowledges the receipt of a SERC/PPARC studentship and travel grants as well as support from NASA Astrophysical Theory Grants NAG5-2864 and NAG5-3111.

REFERENCES

Abell, G. O., Corwin, H. G. & Olowin, R. P., 1989, *Ap. J. Suppl.*, **70**, 1.
 Abell, G. O., 1958, *Ap. J. Suppl.*, **3**, 211.
 Bahcall, N. A. & Cen, R., 1992, *Ap. J. Lett.*, **398**, L81.
 Bahcall, N. A. & Soneira, R. M., 1983, *Ap. J.*, **270**, 20.
 Bahcall, N. A. & West, M., 1992, *Ap. J.*, **392**, 419.
 Bogart, R. S. & Wagoner, R. V., 1973, *Ap. J.*, **181**, 609.
 Croft, R. A. C. & Efstathiou, G., 1994, *Mon. Not. R. astr. Soc.*, **267**, 390.
 Croft, R. A. C. & Efstathiou, G., 1995, In: *Proceedings of the 11th Potsdam Cosmology Workshop*, ed. Muecket, J., World Scientific.
 da Costa, L. N., Geller, M. J., Pellegrini, P. S., Latham, D. W., Fairall, A. P., Marzke, R. O., Willmer, C. N. A., Huchra, J. P., Calderon, J. H., Ramella, M. & Kurtz, M. J., 1994, *Ap. J. Lett.*, **424**, L1.
 Dalton, G. B., Efstathiou, G., Maddox, S. J. & Sutherland, W. J., 1992, *Ap. J. Lett.*, **390**, L1 (**DEMS92**).
 Dalton, G. B., Croft, R. A. C., Efstathiou, G., Sutherland, W. J., Maddox, S. J. & Davis, M., 1994a, *Mon. Not. R. astr. Soc.*, **271**, L47.
 Dalton, G. B., Efstathiou, G., Maddox, S. J. & Sutherland, W. J., 1994b, *Mon. Not. R. astr. Soc.*, **269**, 151.
 Dalton, G. B., Efstathiou, G., Sutherland, W. J., Maddox, S. J. & Davis, M., 1997, *Mon. Not. R. astr. Soc.*, , *submitted*.
 Davis, M. & Peebles, P. J. E., 1983, *Ap. J.*, **267**, 465.
 Dekel, A., Blumenthal, G. R., Primack, J. R. & Olivier, S., 1989, *Ap. J. Lett.*, **338**, L5.
 Efstathiou, G., Dalton, G. B., Sutherland, W. J. & Maddox, S. J., 1992, *Mon. Not. R. astr. Soc.*, **257**, 125 .
 Efstathiou, G., Sutherland, W. J. & Maddox, S. J., 1990, *Nature*, **348**, 705.
 Eke, V., Cole, S., Frenk, C. S. & Navarro, J., 1996, *Mon. Not. R. astr. Soc.*, **281**, 703.
 Hamilton, A. J. S., 1993, *Ap. J. Lett.*, **406**, L47.
 Hauser, M. G. & Peebles, P. J. E., 1973, *Ap. J.*, **185**, 757.
 Huchra, J. P., Henry, P., Postman, M. & Geller, M. J., 1990, *Ap. J.*, **365**, 66.
 Klypin, A. A. & Kopylov, A. I., 1983, *Sov. Astron. Lett.*, **9**, 41.
 Klypin, A., Holtzman, J., Primack, J. & Regos, E., 1993, *Ap. J.*, **416**, 1.
 Lumsden, S. L., Nichol, R. C., Collins, C. A. & Guzzo, L., 1992, *Mon. Not. R. astr. Soc.*, **258**, 1.
 Mann, R. G., Heavens, A. F. & Peacock, J. A., 1993, *Mon. Not. R. astr. Soc.*, **263**, 798.
 Marshall, H. L., Avni, Y., Tananbaum, H. & Zamorani, G., 1983, *Ap. J.*, **269**, 35.

Mo, H. J., Jing, Y. P. & White, S. D. M., 1996, *Mon. Not. R. astr. Soc.*, , *submitted*.
 Nichol, R. C., Briel, U. G. & Henry, J. P., 1994, *Mon. Not. R. astr. Soc.*, **267**, 771.
 Nichol, R. C., Collins, C. A., Guzzo, L. & Lumsden, S. L., 1992, *Mon. Not. R. astr. Soc.*, **255**, 21P.
 Peacock, J. A. & West, M. J., 1992, *Mon. Not. R. astr. Soc.*, **259**, 494.
 Peebles, P. J. E., 1980, *The Large Scale Structure of the Universe*, Princeton University Press.
 Postman, M., Huchra, J. P. & Geller, M. J., 1992, *Ap. J.*, **384**, 404 (**PHG**).
 Romer, A. K., Collins, C., MacGillivray, H., Cruddace, R. G., Ebeling, H. & H.Boringer, 1994, *Nature*, **372**, 75.
 Sutherland, W. J. & Efstathiou, G., 1991, *Mon. Not. R. astr. Soc.*, **248**, 159.
 Sutherland, W. J., 1988, *Mon. Not. R. astr. Soc.*, **234**, 159.
 Tonry, J. & Davis, M., 1979, *Ap. J.*, **84**, 1511.
 Wright, E. L., Smoot, G. F., Kogut, A., Hinshaw, G., Tenorio, L., Lineweaver, C., Bennett, C. L. & Lubin, P. M., 1994, *Ap. J.*, **420**, 1.